Efficient Sampling of Bacterial Signal Transduction for Detection of Pulse-Amplitude Modulated Molecular Signals

A. Ozan Bicen, *Student Member, IEEE*, Caitlin M. Austin, Ian F. Akyildiz, *Fellow, IEEE*, and Craig R. Forest

***Abstract*—The sampling of the bacterial signal transduction is investigated for molecular communication (MC). It is assumed that the finite-duration amplitude modulated, i.e., pulse-amplitude modulated (PAM), concentration of a certain type of molecule is used for information transmission. The bacterial signaling pathway is modified to transduce the input molecules to the output signal, i.e., produce green fluorescent protein (GFP). The bacterial signal transduction is composed of a set of biochemical reactions which impose randomness on the response. Therefore, the input-output relation, the timing issues, and the noise effects for the bacteria response are characterized based on both analytical and experimental observations. Sampling schemes for the raw bacteria response are proposed based on the total response duration, the peak value, the ramp-up slope, and the ramp-down slope. Each sampling scheme is shown to be providing a one-to-one and monotonic function of the input. The sampling based on the ramp-up slope is shown to be statistically favorable for the detection of PAM molecular signals. Accordingly, the time interval selection and non-coherent sampling are studied for the efficient calculation of the ramp-up slope from the raw bacteria response. This work provides a basis for the sampling of the raw bacteria response and enables accurate detection of PAM molecular signals via bacterial response for MC and sensing applications.**

***Index Terms*—Bacterial signal transduction, detection, microfluidics, molecular communication, systems biology.**

I. Introduction

THE envisioned applications of molecular communication (MC) have originated research on the utilization of the available signaling mechanisms in the cells for information transmission. MC is ubiquitous in biological systems including populations of microorganisms and organs [1], [2]. For example, bacteria form biofilms and exchange signals to initiate gene expression based on the population density, i.e., quorum sensing. Molecular signals are also present in multicellular organisms, e.g., hormones and neurotransmitters are used to regulate physiological activities. Genetic engineering of cells, specifically bacteria, has been prompted to develop molecular oscillators and transceivers for the information transmission using molecular signals [3]–[6]. The study of bacteria and its response to the external environment is critical for understanding cellular response due to the relative ease of engineering and testing, which already gained a wide attention in the literature for sensing and monitoring [7]–[11]. The goal of this paper is to determine how the synthetic bacteria respond to external variation in a molecular signal, e.g., in concentration of a certain type of molecule, by signal transduction and how this variation can be detected based on the bacteria response, e.g., green fluorescent protein (GFP) illumination. We, first, examine the raw bacteria response both theoretically and experimentally for the one-to-one input-output relation, the noise, and the timing of the bacterial signal transduction. We, second, investigate statistically the sampling of the bacteria response as the received signal and the detection of the molecular signals. We consider one molecular source releasing finite duration concentration signals with a specific type of molecule, i.e., pulse-amplitude modulation (PAM), and a single bacterial receiver. The information is modulated onto the amount of the specific molecule in the concentration, which the bacteria cannot synthesize.

The molecular propagation have been extensively studied and can be found in many works [12]–[15]. The information-theoretic fundamental limits related to MC are analyzed in [16]–[18]. A commonly taken approach is to consider nanomachines equipped with nanoscale molecular sensors that are capable of measuring received concentration [19], [20]. The undergoing biochemical processes for transmission and reception of molecular signals in the synthetic biological transceivers and their signal transduction pathways prove much more difficult to model and circumscribe [21]–[24]. The challenge on which we concentrate in this paper is the effect of the signal transduction on the sampling of the continuous output signal in MC systems with bacterial receivers. Of particular interest is the issue of the effect of the noise and the timing on the detection of the PAM molecular signal. The issues of the signal transduction in cells have been broadly reviewed and can be found in many books ([25], Chapter 2), ([26], Chapter 24), ([27], Chapter 5), ([28], Chapter 2). The biochemical modeling of the signal transduction has been often studied in the context of reaction-rate equations (RRE). Different cases have been

Manuscript received February 28, 2015; revised June 05, 2015; accepted July 16, 2015. Date of publication September 11, 2015; date of current version September 22, 2015. This work was supported by the U.S. National Science Foundation (NSF) under the Grant CNS-1110947. This paper was recommended by Associate Editor R. Sarpeshkar.

A. O. Bicen and I. F. Akyildiz are with the Broadband Wireless Networking Laboratory (BWN-Lab), School of Electrical and Computer Engineering, Georgia Institute of Technology, Atlanta, GA 30332 USA (e-mail: bozan@ece.gatech.edu; ian@ece.gatech.edu).

C. M. Austin and C. R. Forest are with the Precision Biosystems Laboratory, School of Mechanical Engineering, Georgia Institute of Technology, Atlanta, GA 30332 USA (e-mail: caitlin.austin@gatech.edu; cforest@gatech.edu).

Color versions of one or more of the figures in this paper are available online at http://ieeexplore.ieee.org.

Digital Object Identifier 10.1109/TBCAS.2015.2465182

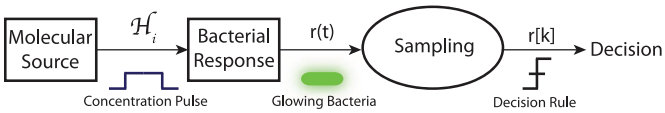

Fig. 1. The block diagram representation of the bacteria-based PAM molecular signal detection system.

considered, among them: the bacterial signal transduction is modeled using a set of RRE to predict the bacteria response in a microfluidic platform [11], or simplification of an RRE model of signal transduction is utilized under quasi-equilibrium condition to design biological circuits with both analog and digital signaling functionalities [29]. Close to our work, [6] investigates performance of pulse-based on-off keying (OOK) modulation, i.e., single bit transmission per pulse, for bacterial receivers, where the binary one is represented by the input signal, and the binary zero is represented by the removal of the input from the channel. Therefore, detection of the multi-level input signals by bacterial signal transduction has been an open problem to date and has not been addressed yet to the best of our knowledge.

The detection block diagram for the considered detection problem is given in Fig. 1. Molecular source releases PAM molecular signals with level $\mathcal{H}_i$. The bacteria transduce the molecular signal to GFP, recorded illumination of which denoted as received signal $r(t)$. The continuous-time received signal $r(t)$ is sampled based on either the peak value, the total response duration, the ramp-up slope, or ramp-down slope, and the discrete-time $r[k]$ is obtained. Finally, thresholding is applied based on the predefined decision rules. Accordingly, the input molecular signal $\mathcal{H}_i$ is decided.

In this paper, we consider the issues of the one-to-one input-ouput relation, noise, and timing in the context of detection via sampling the bacterial signal transduction at the receiver. The transient variations in the noise and timing issues are tightly linked with the sampling of the raw bacteria response. The random jitter in the beginning, peak, and the ending of the bacteria response entails that the sampling of the bacteria response at a fixed instant will be exposed to additional distortion apart from the noise. The noise and the timing together are responsible for the distortion observed on the bacteria response. The following questions are sought to be investigated throughout the course of this work.

- When is the input-output relation one-to-one?
- How does the noise in the bacteria response vary with the time?
- What are the randomness effects on the timing of the response beginning, the peak instant, and the response ending?
- How should the raw bacteria response be sampled to minimize noise and timing effects for the detection of the input molecular signal?

The question regarding the sampling of the bacteria response for the detection of the input signal is principally significant, since the noise and the timing issues of the biological receivers have not been studied empirically for M-ary PAM molecular signals based on the experimental data. Theoretical analysis of biological transceivers has been performed based on RRE models in [29], where the biological noise and the timing issues are neglected. The robust design of biochemical signaling pathways with kinetic parameter uncertainties and external disturbances is studied based on control theory in [30]–[32]. However, the inference of information from the biochemical signal transduction has been an open debate. The provided performance analysis of the on-off keying modulation for bacterial receivers in [6] is only valid for binary PAM with transmission of a fixed level for 1 and transmission of no signal for 0. The sampling of the received signal from raw bacteria response is a subject yet to be studied for M-ary detection in the course of this work.

The remainder of this paper is organized as follows. In Section II, the bacterial signal transduction is theoretically studied. In Section III, the timing and noise issues in the bacteria response is investigated empirically based on experiments from a microfluidic platform. In Section IV, the sampling of the raw bacteria response is discussed, and the statistical characterization is performed. The detection of molecular signals via sampling the ramp-up slope is elaborated in Section V. The final conclusions are provided in Section VI.

II. Bacterial Signal Transduction

The bacteria can generate a controlled response to an external molecular stimuli by signal transduction. For example, the gene sequence of bacteria can be modified such that output protein production can be controlled in response to an input molecular signal ([25], Chapter 2). Here, we provide an overview of the biochemical phenomena of the bacterial response to external stimuli and how it makes the detection of the input signal possible.

To guide the detection of molecular signals, the basics of the input-output relation, e.g., input controlled synthesis of GFP, by bacteria must be first understood. Therefore, the bacterial signal transduction is analytically investigated focusing on the gene expression. In the following subsections, first, the specific model of the bacteria signal transduction is overviewed, and then, the input-output relation of the bacteria response is discussed along with the error analysis.

A. Model

The gene expression is regulated, e.g., activated, by the control of inducer molecules, which are supposed to be externally provided. To analytically study the bacteria response, we focus on the protein production as the *output signal*. The output signal is analyzed with respect to the externally provided inducer molecules, which is the *input signal*. Specifically, simplification of the RREs for the gene expression under the quasi steady-state and equilibrium approximations is considered for modeling ([28], Chapter 2), ([25], Chapter 2). The detailed explanation for the modeling of gene expression and the simplifications of the RREs can be found in ([28], Chapter 2), ([25], Chapter 2). Accordingly, the output signal is related to the input signal via the RRE given by

$$\frac{\partial y(t)}{\partial t} = \frac{\beta x^n}{\theta^n + x^n} - \alpha y(t) \tag{1}$$

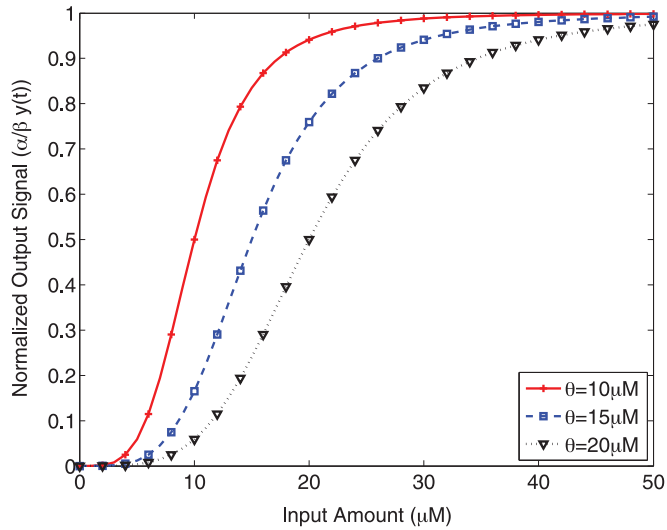

Fig. 2. The input-output relation of the bacteria response based on (4). The activation coefficient θ is taken as 10, 15, and 20 μM, $n = 4$, and the input amount varied from 0 to 50 μM. The output signal is normalized by α/β.

where y is the output signal, x is the input signal level, θ is the activation coefficient. For example, when the expression is significantly activated when $x > \theta$, n determines steepness of the bacteria signal transduction, β is the empirical rate parameter defining the maximum expression level when $x \gg \theta$, and α is the degradation rate of the output signal y. Although this model is a simplified version of the bacterial signal transduction, it captures the input-output behavior of the bacteria response based on the gene expression.

To solve (1) for the step response with the zero initial conditions, i.e., the input is changed from zero to its desired level, Laplace transform of y, i.e., $Y(s) = \mathcal{L}\{y(t)\}$, is used, and after partial fraction decomposition Y is found as

$$Y(s) = \left(\frac{\beta x^n}{\theta^n + x^n}\right)\frac{1}{\alpha}\left(\frac{1}{s} - \frac{1}{s+\alpha}\right). \tag{2}$$

Finally, by taking the inverse Laplace transform of Y, i.e., $y(t) = \mathcal{L}^{-1}\{Y(s)\}$, y is found as

$$y(t) = \frac{\beta x^n}{\alpha(\theta^n + x^n)}(1 - e^{-\alpha t}). \tag{3}$$

B. Input-Output Relation and Error Analysis

To study the input-output relation, the normalized steady-state response of the bacteria is obtained using (3) as

$$\lim_{t\to\infty}\frac{\alpha}{\beta}y(t) = \frac{x^n}{\theta^n + x^n}. \tag{4}$$

In Fig. 2, it is observed that the bacteria response is a one-to-one function of the input within an acceptable range. For example, when input is in the range from 15 to 25 μM for $\theta = 20$ μM in Fig. 2, the output can even be approximated as a linear function of the input. As the input signal level kept increasing, the bacteria response is observed to be saturating in Fig. 2. After saturation, the further increasing the input signal makes no difference on the output signal, i.e., input signal is indistinguishable based on the output signal. On the other hand, the output signal stays approximately zero for small input values, e.g., a few μM in Fig. 2. However, when the input signal range is kept both sufficiently large and below saturation level, a one-to-one input-output relation can be achieved.

We also analytically study the transient response of the bacteria to point out the impact of error in the maximum expression level β. To this end, the linear approximation of the $y(t)$ in (3) for $t = 0$ is used. First order Taylor series expansion of the exponential term, i.e., $e^{-\alpha t} \approx 1 - \alpha t$ for $\alpha t \approx 0$, gives

$$y(t) \approx \frac{x^n}{(\theta^n + x^n)}\beta t \tag{5}$$

where the term $x^n/(\theta^n + x^n)$ is constant with respect to time. We define $\hat{\beta} = \beta + \epsilon$ as the erroneous version of the maximum production level β, and ϵ incorporates the arbitrary error factor. Accordingly, the erroneous output $\hat{y}(t)$ can be rewritten by plugging $\hat{\beta}$ into (5) as

$$\begin{aligned}\hat{y}(t) &= \frac{x^n}{(\theta^n + x^n)}\beta t + \frac{x^n}{(\theta^n + x^n)}\epsilon t \\ &= y(t) + \frac{x^n}{(\theta^n + x^n)}\epsilon t.\end{aligned} \tag{6}$$

The absolute error in the output, i.e., $|\hat{y}(t) - y(t)|$, is

$$|\hat{y}(t) - y(t)| = \frac{x^n}{(\theta^n + x^n)}\epsilon t. \tag{7}$$

Note that the error term evolves with time. Accordingly, the error on the output is expected to increase during the ramp-up behavior of the bacteria response, i.e., the impact of erroneous protein production rate $\hat{\beta}$ on the output is more severe as time elapses. In the next section, we will investigate the bacteria signal transduction experimentally for PAM molecular signals.

III. Experimental Analysis of Bacteria Response

We perform tests with *Escherichia coli* (*E. coli*) bacteria strains on a microfluidic platform [6], [11]. The microfluidic platform provides control over the input molecular signal, i.e., the concentration pulse level and duration. Furthermore, the microfluidic platform hosts bacteria strains in chambers, where a microfluidic channel with flow carries the media composed of both the required nutrients and the input signal (Fig. 3).

The *E. coli* bacteria are genetically engineered to express genes from the autoinducer system of *Vibrio fischeri* (*V. fischeri*) bacteria and produce a variant of the green flouresence protein (GFP) under the presence of the autoinducer N-Acyl homoserine lactone (AHL) molecules. The produced GFP represents the bacteria response, i.e., output signal, and measured using the fluorescence microscopy. The autoinducer AHL molecules represent the input signal. Since the *E. coli* bacteria cannot encode the genes to produce AHL, the output signal can be utilized to detect the amplitude of the externally provided

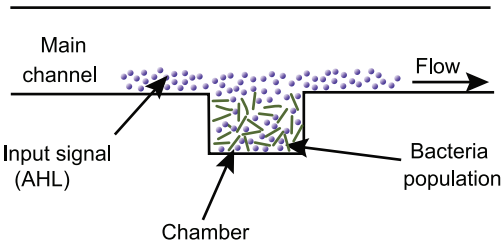

Fig. 3. The chamber that is connected to the microfluidic channel and hosts the genetically-engineered bacteria.

PAM molecular signal, i.e., the level of a finite duration AHL concentration pulse.

The specifics of the experimental system composed of the genetically engineered *E. coli* bacteria and the microfluidic platform were previously presented in [6], [11]. In the preceding discussions, we start with the study of the molecular signal propagation through the microfluidic channel. The negligible propagation delay, and invariance of the pulse amplitude and duration are pointed out for the multiple chambers hosting the bacteria. Then, the timing and the noise issues of the bacteria signal transduction are investigated based on measurements from the experimental platform. We provide a comprehensive look at the raw bacteria response for molecular signal detection and set the stage for statistical comparison of the different strategies for sampling of the raw bacteria response.

A. Pulse Prolongation Between Multiple Chambers

Having bacteria response from the different chambers attached to the same microfluidic channel is useful to obtain multiple measurements and alleviate noise effects on the output signal for detection purposes. The microfluidic channel has a cross-section of 250 μm $\times$ 10 μm, and flow rate is 360 μl/hr. The chambers are placed on the microfluidic channel with a constant separation distance, e.g., 0.5 mm.

To obtain the prolongation of the concentration pulse until it reaches to the chamber k, we first calculate the molecular propagation delay ($\tau_{\text{delay}}^{(k)}$) until the chamber k as [14]

$$\tau_{\text{delay}}^{(k)} = \frac{l_1 + k \cdot l_{\text{sep}}}{u} \tag{8}$$

where l_1 is the distance of the closest chamber to the source, l_{sep} is the separation distance between chambers, and u is the area averaged flow velocity. The dispersion length ($l_{\text{disp}}^{(k)}$) until the chamber k is obtained using the diffusion equation as

$$l_{\text{disp}}^{(k)} = \sqrt{2D\tau_{\text{delay}}^{(k)}} \tag{9}$$

where D is the Taylor dispersion adjusted diffusion constant. Finally, the pulse prolongation duration τ_{prolong} is obtained as

$$\tau_{\text{prolong}}^{(k)} = \frac{l_{\text{disp}}^{(k)}}{u}. \tag{10}$$

The molecular propagation delay and the pulse prolongation durations are tabulated in Table I, which are in the range of a few 10 ms. The calculated delay and prolongation durations are much less compared to the required pulse duration to get a response from the bacteria, which is in the order of 10 min [6], [11].

TABLE I
CONCENTRATION PULSE PROLONGATION THROUGH THE MICROFLUIDIC CHANNEL

	Distance	Delay	Prolongation Duration
Chamber 1	1.16 mm	0.0260 sec	0.0438 sec
Chamber 2	1.66 mm	0.0262 sec	0.0440 sec
Chamber 3	2.16 mm	0.0264 sec	0.0441 sec
Chamber 4	2.66 mm	0.0266 sec	0.0443 sec
Chamber 5	3.16 mm	0.0268 sec	0.0445 sec

The separation distance between the source and the chambers is in the range of a few mm, and the considered pulse durations are in the range of a few 10 min to get response from the bacteria in the experimental microfluidic platform. Accordingly, the input molecular signal can be taken invariant with respect to the propagation through the microfluidic channel. Therefore, the bacteria in different chambers are exposed to the same concentration pulse duration. Furthermore, the delay due to molecular propagation is also negligible since the bacteria response is in the hours scale [11], [29], which will be investigated in the following subsections.

B. Timing Analysis

The timing of the bacterial response behavior has importance to be able to efficiently sample and process the output signal for detection of the amplitude of the PAM molecular signal. The bacterial signal transduction involves ordered set of biochemical reactions. A set of biochemical reactions produces fluctuating number of intermediate molecules in short bursts at random time intervals, which need to reach an effective level to activate the next step in the signal transduction pathway. Therefore, there can be large differences in the time delay required for signal transduction, especially across the bacteria population [21]. Here, we investigate the timing specifically with respect to the response beginning, i.e., the instant that bacteria starts to produce the output signal, and the peak instant, i.e., the moment when the bacteria response reaches its peak, and the total response duration, i.e., the time elapses from the beginning of the bacteria response to the end.

The transient bacteria response behavior for PAM molecular signals of 15, 20, 22.5 μM is shown in Fig. 4, which are averaged over 4, 7, and 5 experiments, respectively. The reason for the different number of measurements for the different concentration inputs is as follows. Once loaded, a few bacteria will settle in the trapping chambers. Not all chambers will have bacteria in them, which means the number of measurements can change from experiment to experiment. The molecular signals have a finite duration of 50 min.

The output signal is the relative fluorescence illumination. Fluorescent images were captured once every 10 min and post-processed using MATLAB. The intensity of the pixels within the bacteria chamber was averaged and the background fluorescence was subtracted, yielding the relative fluorescence (arbitrary units, or a.u.). Each run represents a single chamber that was imaged over time. Each data point for that run is calculated

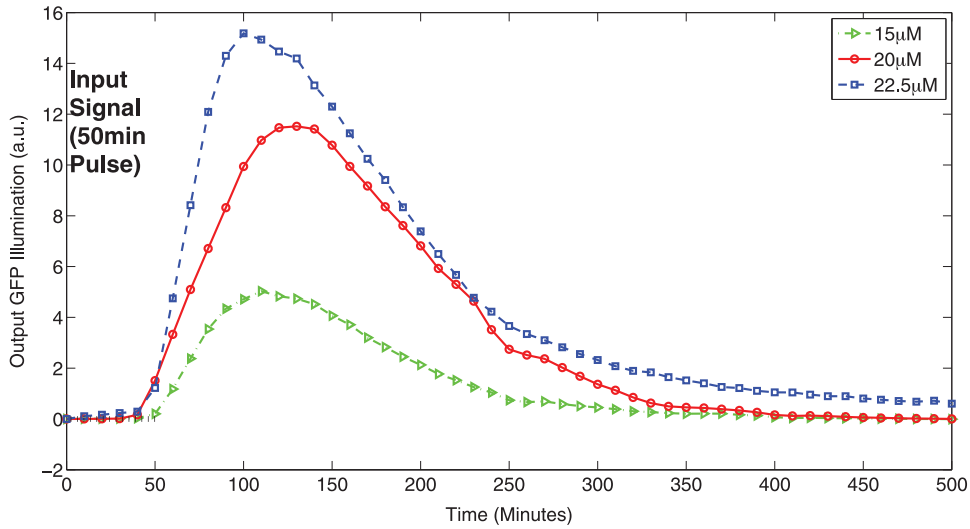

Fig. 4. The transient response of the bacteria for different PAM molecular signal amplitudes.

using the image processing mentioned above. The average for a concentration represents the averaging of all runs for that concentration. Therefore the standard deviations are the deviations between the individual chambers.

1) Bacteria Response Beginning: The difference of the response beginning and input molecular signal start $(t = 0)$ times in Fig. 4 gives the bacteria response beginning delay. The response beginning delay is shown to be depending on the input molecular signal amplitude in Fig. 4. For 22.5 μM and 20 μM, the mean response beginning delay is shown to be converging and less than the one for 15 μM. The input dependent beginning time of the bacteria response makes the sampling of the output signal at that particular instant challenging. Furthermore, since the response beginning delay is not always providing a one-to-one input-output relation as the input signal amplitude is further increased, it is not an efficient option for the detection of PAM molecular signals. For example, consider 2 a.u. is selected as the reference to decide on the beginning of the bacteria response, the response reaches the output level of 2 a.u. at the same instant for both input levels of 20 μM to 22.5 μM.

2) Peak Instant: The peak time of the bacteria response behavior is shown to be varying based on the amplitude of the input molecular signal in Fig. 4. Furthermore, the input dependance of the peak time is observed to be non-monotonic. Therefore, determination of a fixed time instant for sampling of the peak of the bacteria response is not trivial. For example, the peak instant for the input level 20 μM is later than both 22.5 μM and 15 μM input levels. The experimental data in Fig. 4 suggest that the tight timing requirements on the sampling of the bacteria response is not favorable, since the bacteria response behavior is not synchronized to the input signal source.

3) Total Response Duration: Lastly, the total response duration, i.e., the time elapses form the beginning of the response to the ending, is observed in Fig. 4. The total response duration increases monotonically with input molecular signal amplitude. Furthermore, the total response duration is shown to be providing a one-to-one relation between the input and output in in Fig. 4. The use of the total response duration for sampling of the received signal and the detection of the input PAM molecular signal is further discussed in Section IV.

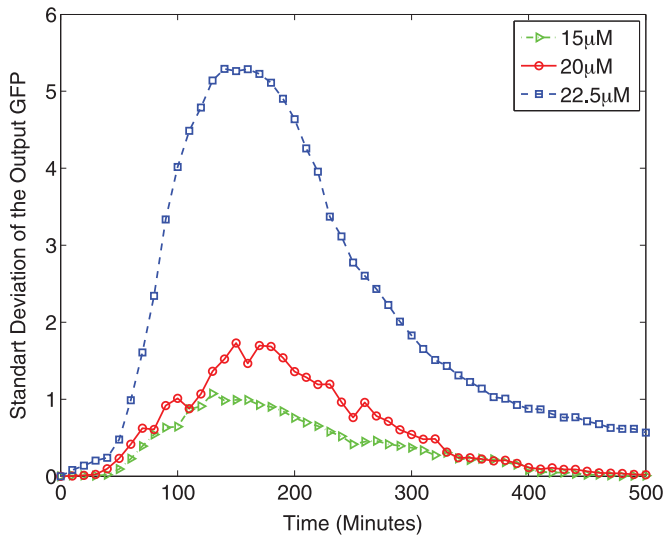

Fig. 5. The standard deviation of the bacteria response with respect to time for different PAM molecular signal amplitudes.

C. Transient Noise Analysis

In Fig. 4, the bacteria response behavior is identified to be composed of three regions, i.e., ramp-up region which takes place from beginning of the response to the peak, peak region where the response reaches its peak value, and the ramp-down region which takes place from the peak to the end of response. Here, the impact of noise on the bacteria response during ramp-up, peak, and ramp-down regions is studied. To this end, the standard deviation of the bacteria response behavior with respect to time for PAM molecular signals of 15, 20, and 22.5 μM is shown in Fig. 5.

The higher standard deviation implies higher noise effect on the output signal. The standard deviation of the response is observed to be increasing as it reaches its peak in the ramp-up region. Then, the standard deviation of the response decays until

the response ends. For different input levels, i.e., 15, 20, and 22.5 μM, the same trend in the bacteria response behavior is observed in Fig. 5. Increasing noise from the response beginning to the peak in the ramp-up region conforms with the theoretical insights provided in Section II.B. In (6), the absolute error in the output signal, i.e., $|\hat{y}(t) - y(t)|$, due to the error ϵ in the maximum protein production level β is identified to be increasing over time t. In the line with our theoretical investigations, it is shown experimentally that the increase in the output protein amount yields increased error contribution in the output, i.e., the error in the output signal is amplified as it reaches to the peak response value.

The study of the stochasticity in the gene expression has recently been a research field of interest [22], [33]. The impact of perturbation, i.e., stimulus, on the noise in the signal transduction is investigated in [33], and directly proportional scaling of the noise variance with the protein abundance is reported, which are normalized with respect to the pre-stimulus values. Similarly, in Fig. 5, it is observed that the standard deviation of the bacteria response increases proportional to the magnitude of the response, i.e., standard deviation increases as the input level is increased from 15 μM to 22.5 μM. Next, the different sampling strategies of the received signal are investigated to facilitate accurate and timely detection of the PAM molecular signals.

IV. Sampling of the Received Signal Based on the Bacterial Signal Transduction

So far, both analytical and experimental characterizations of the bacteria response are performed. However, the sampling of the received signal, i.e., mapping of the recorded raw bacteria response to the decision space, is missing such that the PAM input signal can be detected accurately. The input signal can be detected via applying thresholding on the received signal, i.e., comparing the received signal with the predefined thresholds for different input signal amplitudes. In this section, we extend our theoretical and experimental analyses in the former sections by proposing and comparing four different sampling strategies for the raw bacteria response, namely, the total response duration, the peak level of the response, the ramp-up slope, and the ramp-down slope.

A. Sampling Strategies for the Raw Bacteria Response

In the following, we study the sampling of the received signal $(r_k(t))$ from the raw bacteria response based on the total response duration $(r_{\text{total}}[k])$, the peak value $(r_{\text{peak}}[k])$, ramp-up slope $(r_{\text{up}}[k])$, and the ramp-down slope $(r_{\text{down}}[k])$. The sample sample index k indicates the kth transmission of the PAM molecular signal. It should be noted that while the received signal $r_k(t)$ from the bacteria response is a continuous function of t, the sampled responses $r_{\text{total}}[k], r_{\text{peak}}[k], r_{\text{up}}[k], r_{\text{down}}[k]$ are discrete-time and a function with sample index k. The one-to-one input-output relation of the different sampling strategies is specifically investigated for the detection purposes.

To sample the raw bacteria response $r(t)$ for the total response duration $r_{\text{total}}[k]$, the duration between the instant when the response exceeds a predefined threshold η_{total} and the instant the response goes below the threshold η_{total} is used, which is given by

$$r_{\text{total}}[k] = \sup_t \arg\min_t |r_k(t) - \eta_{\text{total}}| - \inf_t \arg\min_t |r_k(t) - \eta_{\text{total}}|. \quad (11)$$

For evaluations, we set the threshold for output flouresence illumination to $\eta_{\text{total}} = 1$ a.u., i.e., the response beginning is taken as the instant when the measured bacteria response exceeds $\eta_{\text{total}} = 1$ a.u. and the response ending is taken as the instant when the measured bacteria response reduces below $\eta_{\text{total}} = 1$ a.u. The peak value is taken as the maximum of the raw bacteria response as

$$r_{\text{peak}}[k] = \sup_t r_k(t). \quad (12)$$

Apart from the total response duration and the peak value, the slope of the ramp-up and the ramp-down behavior in the bacteria response can also be utilized to decide on the input signal level. Accordingly, ramp-up slope $r_{\text{up}}[k]$ can be calculated as

$$r_{\text{up}}[k] = \frac{r_k(t_2) - r_k(t_1)}{t_2 - t_1}. \quad (13)$$

The ramp-up slope is calculated for the interval of $t_1 = 60$ and $t_2 = 70$ mins. The ramp-down slope is calculated as

$$r_{\text{down}}[k] = \frac{r_k(t_2) - r_k(t_1)}{t_2 - t_1} \quad (14)$$

where we use the interval of $t_1 = 160$ and $t_2 = 170$ mins for the evaluations.

The mean of the sampled received signal using total response duration, the peak value, the ramp-up slope, and the ramp-down slope are shown in Figs. 6, 7, 8, and Fig. 9, respectively, with respect to different input signal levels. It should be noted that the received signal is in different units for different sampling strategies, i.e., minutes for the total response duration, a.u. for the peak value, and a.u./mins for the slope of ramp-up and the ramp-down. It is observed that there is a one-to-one relation between the received signal and the input signal for all four sampling strategies of the received signal. Furthermore, the mean of the received signal monotonically increases as the input level increased for all four strategies of the received signal, which enables non-overlapping mapping of the received signal to the decision space. The input signal can be detected via comparison of the received signal with the predetermined thresholds based on the selected sampling strategy. However, each sampling strategy yields different statistical properties for the sampled received signal, i.e., mean and variance. Therefore, in the next subsection, we study the distinguishability of the sampled received signals to detect distinct input levels.

B. Statistical Distinguishability

Here, the detection performance of the four sampling strategies for the received signal are statistically compared. We utilize

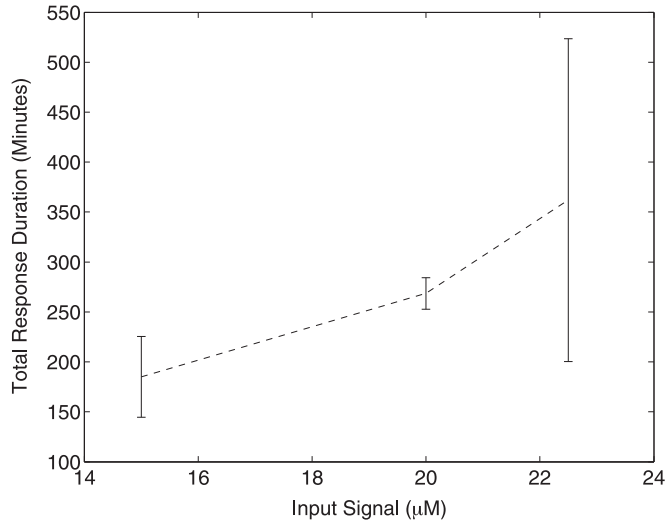

Fig. 6. Input-output relation for the sampling of the received signal using total response duration.

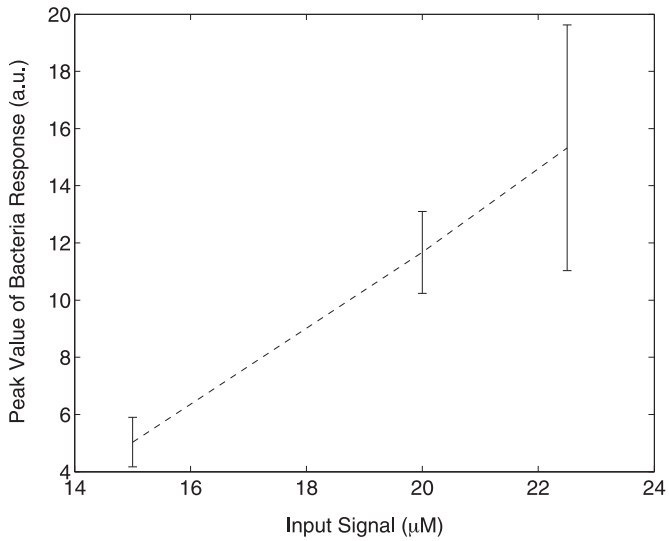

Fig. 7. Input-output relation for the sampling of the received signal using the peak value.

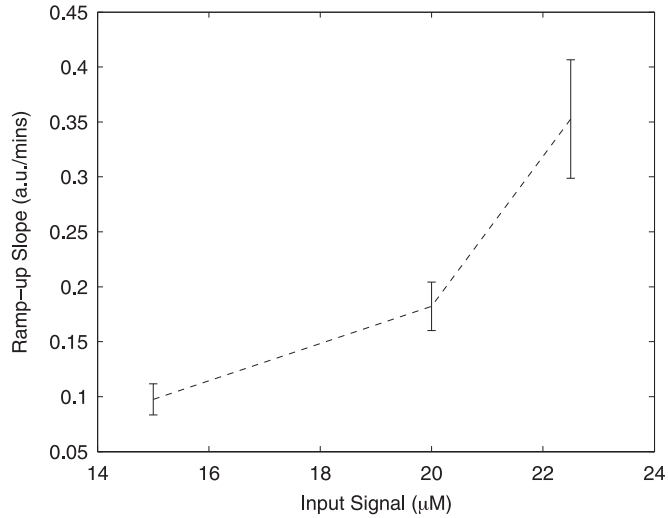

Fig. 8. Input-output relation for the sampling of the received signal using the ramp-up slope.

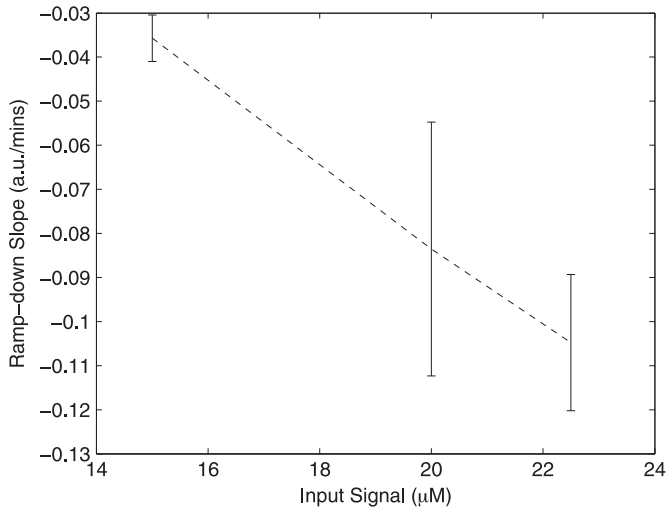

Fig. 9. Input-output relation for the sampling of the received signal using ramp-down slope.

the t-test with unequal variances ([34], Chapter 4), where obtained samples from the raw bacteria response are assumed to be normally distributed. The probability that the obtained two samples are belonging to the same input level, i.e., p-value, is specifically studied. The smaller the p-value, the more **unlikely** the compared samples are belonging to the same input signal level. In the following, the obtained p-values are examined for the decision between the different input level pairs.

The p-values are tabulated in Table II. For decision between 15 μM and 20 μM, the lowest p-values are provided by peak value and the ramp-up slope, i.e., $5.68 \cdot 10^{-6}$ and $3.41 \cdot 10^{-5}$, respectively, where the later one is 6 times larger than the former. For the decision between 15 μM and 22.5 μM, the lowest p-value is provided by the ramp-up and the ramp-down slope, i.e., $2.35 \cdot 10^{-4}$ where the p-value by sampling the peak is about 20 times larger than them. For the decision between 20 μM and 22.5 μM, the lowest p-value, i.e., $1.17 \cdot 10^{-3}$, is provided by the ramp-up slope, where the other interpretations

TABLE II
p-VALUES FOR THE SAMPLING STRATEGIES OF THE RECEIVED SIGNAL

Sampling Scheme	$\mathbf{15-20}$ μ**M**	$\mathbf{15-22.5}$ μ**M**	$\mathbf{20-22.5}$ μ**M**
Total Response Duration	$2.11 \cdot 10^{-2}$	$6.91 \cdot 10^{-2}$	0.266
Peak Value	$5.68 \cdot 10^{-6}$	$4.9 \cdot 10^{-3}$	0.131
Ramp-up slope	$3.41 \cdot 10^{-5}$	$2.35 \cdot 10^{-4}$	$1.17 \cdot 10^{-3}$
Ramp-down slope	$4.1 \cdot 10^{-3}$	$2.11 \cdot 10^{-4}$	0.131

of the bacteria response have an approximately 100 times larger p-value. On the other hand, the total response duration provides the worst performance for detection purposes as a sampling strategy of the received signal based on the p-value results.

While the ramp-up slope and the peak value provides a close p-value for the decision between 15 μM and 20 μM, the p-value of the input pulse pairs is further amplified as the input levels are increased, i.e., the peak value has the third smallest p-value for the other input combinations. Meanwhile, the ramp-up slope performs either the lowest or the second lowest p-value.

TABLE III
MEAN (μ) OF THE SAMPLED BACTERIA RESPONSE

Sampling Scheme (unit)	15μM	20μM	22.5μM
Total Response Duration (mins)	185	268	362
Peak Value (a.u.)	5.03	11.66	15.32
Ramp-up Slope (a.u./mins)	0.097	0.18	0.35
Ramp-down Slope (a.u./mins)	-0.035	-0.083	-0.1

TABLE IV
VARIANCE (σ^2) OF THE SAMPLED BACTERIA RESPONSE

Sampling Scheme (unit^2)	15μM	20μM	22.5μM
Total Response Duration (mins^2)	1630	247	26100
Peak Value (a.u.^{2})	0.75	2.04	18.48
Ramp-up Slope (a.u.^{2}/mins^2)	0.00019	0.00048	0.0029
Ramp-down Slope (a.u.^{2}/mins^2)	0.000027	0.00082	0.00023

Based on the statistical analysis of the received signal interpretations in Table II and the experimental transient analysis of standard deviation in Fig. 5, as well as theoretical insights provided in (6), the ramp-up slope is selected to be further investigated for the sampling of the received signal among others in Section V.

C. Probability of Error for Detection of Binary and 3-Ary PAM

The probability of error for the PAM molecular signals is studied with respect to the four sampling schemes. Each different input pulse level $\mathcal{H}_i$ has a specified different mean sampled received signal level μ_i. We assume the sampled received signal for each different $\mathcal{H}_i$ is corrupted by Gaussian noise, i.e.,

$$p(r|\mathcal{H}_i) \sim \mathcal{N}\left(\mu_i, \sigma_i^2\right) \tag{15}$$

where index k is dropped from the sampled bacteria response r for the ease of notation, and σ_i^2 is the variance of the sampled response. The obtained μ_i and σ_i^2 values from experimental measurements are given in Tables III and IV, respectively, for the four sampling schemes.

In the following, we, first, give the formulation of the probability of error for the detection of the binary and the 3-ary PAM molecular signals ([35], Chapter 2). Then, we investigate the detection performance of the four sampling strategies based on the data obtained from experimental measurements for the bacterial signal transduction.

1) Binary Transmission: For the binary transmission case, only two different signal levels, i.e., $\mathcal{H}_1$ and $\mathcal{H}_2$, are considered to be transmitted. During the formulation, the corresponding signal level to $\mathcal{H}_1$ is taken to be lower than the one for $\mathcal{H}_2$. In the line with signal levels, the bacteria response corresponding to $\mathcal{H}_1$ is lower than $\mathcal{H}_2$, e.g., consider the bacteria response for 15 μM and 20 μM in Fig. 4. In Fig. 10(a), the signal points for the binary PAM signals is shown.

We should note again that r is a scalar value and corresponds to obtained received signal via sampling the bacteria response using one of the four sampling strategies. The probability distribution of the received signal for $\mathcal{H}_1$ is as

$$p(r|\mathcal{H}_1) = \frac{1}{\sqrt{2\pi\sigma_1^2}} e^{-\frac{(r-\mu_1)^2}{2\sigma_1^2}} \tag{16}$$

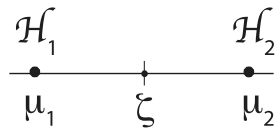

(a)

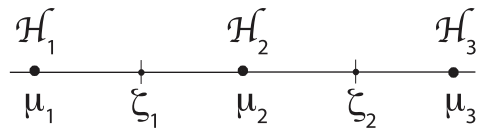

(b)

Fig. 10. The signal points for binary and 3-ary PAM signals in (a) and (b), respectively.

and for the transmission signal level corresponding to $\mathcal{H}_2$, the distribution of the received signal is given as

$$p(r|\mathcal{H}_2) = \frac{1}{\sqrt{2\pi\sigma_2^2}} e^{-\frac{(r-\mu_2)^2}{2\sigma_2^2}}. \tag{17}$$

The probability of error for $\mathcal{H}_1$, i.e., the received signal is greater than the detection threshold ζ, is given by

$$P(r > \zeta|\mathcal{H}_1) = \int_{\zeta}^{\infty} p(r|\mathcal{H}_1) \tag{18}$$

and similarly the probability of error for $\mathcal{H}_2$ is given by

$$P(r < \zeta|\mathcal{H}_2) = \int_{-\infty}^{\zeta} p(r|\mathcal{H}_2). \tag{19}$$

The transmission of both signal levels are taken to be equally likely, and hence, the probability of error for binary PAM is obtained using (18) and (19) by

$$P_b = P(r > \zeta|\mathcal{H}_1) + P(r < \zeta|\mathcal{H}_2). \tag{20}$$

2) 3-Ary Transmission: In 3-ary PAM, the transmission of 3 different pulse amplitudes, i.e., $\mathcal{H}_1$, $\mathcal{H}_2$, and $\mathcal{H}_3$, are considered. We assume corresponding bacteria responses to $\mathcal{H}_1$, $\mathcal{H}_2$, and $\mathcal{H}_3$ are sorted in the ascending order. In Fig. 10(b), signal points for the 3-ary PAM is shown. For the 3-ary transmission case, i.e., three transmission levels, the formulation of the $p(r|\mathcal{H}_1)$ and $p(r|\mathcal{H}_2)$ follows (16) and (17) in the binary case. For $\mathcal{H}_3$, $p(r|\mathcal{H}_3)$ is as

$$p(r|\mathcal{H}_3) = \frac{1}{\sqrt{2\pi\sigma_3^2}} e^{-\frac{(r-\mu_3)^2}{2\sigma_3^2}}. \tag{21}$$

The probability of error for $\mathcal{H}_1$, i.e., $P(r > \zeta_1|\mathcal{H}_1)$ is

$$P(r > \zeta_1|\mathcal{H}_1) = \int_{\zeta_1}^{\infty} p(r|\mathcal{H}_1). \tag{22}$$

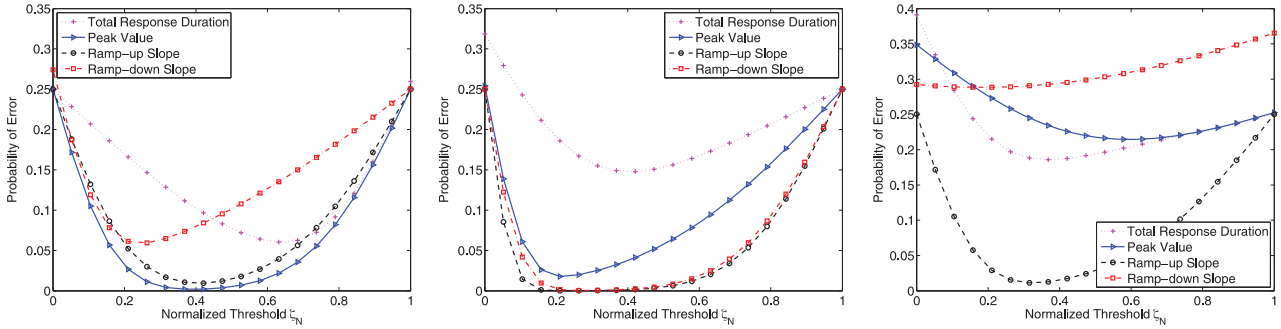

Fig. 11. Comparison of the sampling schemes with respect to probability of error for binary PAM. Input pairs of 15–20 μM (a), 20–22.5 μM (b), and 20–22.5 μM (c) with 50 mins pulse width are considered. Threshold ζ is varied. To present results for different sampling schemes in the same plot, the threshold ζ is normalized using $\zeta_N = (\zeta - \mu_1)/(\mu_2 - \mu_1)$.

The probability of error for $\mathcal{H}_2$, i.e., $P(r < \zeta_1 \cup r > \zeta_2 | \mathcal{H}_2)$ is given as

$$P(r < \zeta_1 \cup r > \zeta_2 | \mathcal{H}_2) = \int_{-\infty}^{\zeta_1} p(r|\mathcal{H}_2) + \int_{\zeta_2}^{\infty} p(r|\mathcal{H}_2). \quad (23)$$

Lastly, the probability of error for $\mathcal{H}_3$, i.e., $P(r < \zeta_2 | \mathcal{H}_3)$, is as

$$P(r < \zeta_2 | \mathcal{H}_3) = \int_{-\infty}^{\zeta_2} p(r|\mathcal{H}_3). \quad (24)$$

With equal transmission probability for all three levels, probability of error for 3-ary PAM is obtained using (22), (23) and (24) as

$$P_b = \frac{1}{3} P(r > \zeta_1 | \mathcal{H}_1) + \frac{1}{3} P(r < \zeta_1 \cup r > \zeta_2 | \mathcal{H}_2) + \frac{1}{3} P(r < \zeta_2 | \mathcal{H}_3). \quad (25)$$

In the following, we present results on probability of error for both binary and 3-ary PAM cases.

3) Discussion: In Fig. 11, the probability of error is evaluated for the binary PAM. The threshold ζ to decide between different input levels $\mathcal{H}_1$ and $\mathcal{H}_2$ is varied between the corresponding specified mean sampled response levels μ_1 and μ_2. Since the threshold ζ has a different unit and scale for each sampling scheme, it is normalized to the interval $[0, 1]$.

For the input level pairs of 15–20 μM, 15–22.5 μM, and 20–22.5 μM, the sampling based on the peak value and the ramp-up slope is shown to be achieving lower error probability than the sampling based on the ramp-down slope and the total response duration in Fig. 11(a), (b), and (c), respectively. The minimum probability of error achieved by each sampling scheme for the binary PAM is given in Table V. For the input level pair of 15–20 μM, sampling based on the peak value achieves the lowest probability of error, i.e., 0.002, whereas the probability of error for sampling based on ramp-up slope is 0.0095. For the input pairs of 15–22.5 μM and 20–22.5 μM, the minimum probability of error is achieved by sampling based on ramp-up slope, which outperforms peak value sampling by 100x and 10x in terms of probability of error, respectively. Additionally, the selection of proper threshold ζ is essential to minimize the probability of error as observed in Fig. 11.

TABLE V
MINIMUM PROBABILITY OF ERROR FOR BINARY PAM

Sampling Scheme	$15-20$ μM	$15-22.5$ μM	$20-22.5$ μM
Total Response Duration	0.0605	0.1478	0.1859
Peak Value	0.002	0.0178	0.2147
Ramp-up Slope	0.0095	0.0001	0.0114
Ramp-down Slope	0.0595	0.0004	0.2885

For 3-ary PAM, all experimentally tested input levels, i.e., 15 μM, 20 μM, and 22.5 μM are allowed to be transmitted. The results on error probability for the four sampling schemes are presented with respect to the normalized threshold ζ_1, which is to decide between $\mathcal{H}_1$ and $\mathcal{H}_2$, and normalized threshold ζ_2, which is to decide between $\mathcal{H}_2$ and $\mathcal{H}_3$, in Fig. 12(a), and (b), respectively. The sampling based on the ramp-up slope is shown to be achieving the lowest error probability compared to the other sampling schemes for the all evaluated choices for the detection thresholds ζ_1 and ζ_2 in Fig. 12(a) and (b), respectively. The minimum probability of error achieved by each sampling scheme for the 3-ary PAM is given in Table VI. The sampling via ramp-up slope achieves more than 5x and 10x improvement in the probability of error over the sampling based on peak value for both studies with respect to the detection thresholds ζ_1 and ζ_2, respectively. The proper selection of the detection thresholds ζ_1 and ζ_2 is essential to optimize the detection performance.

D. Response Observation Duration

The required observation duration on the bacteria response is discussed in the descending order for the four sampling strategies of the received signal. To determine the total response duration, bacteria response needs to end, thus, it has the longest observation duration with respect to the other interpretations of the received signal. The ramp-down slope requires the bacteria response to be in the decay behavior, hence, it requires less observation duration than the total response. However, the required observation duration is still longer than the one for peak value. To sample the peak value, the bacteria response needs to reach its maximum value which happens before the decay behavior

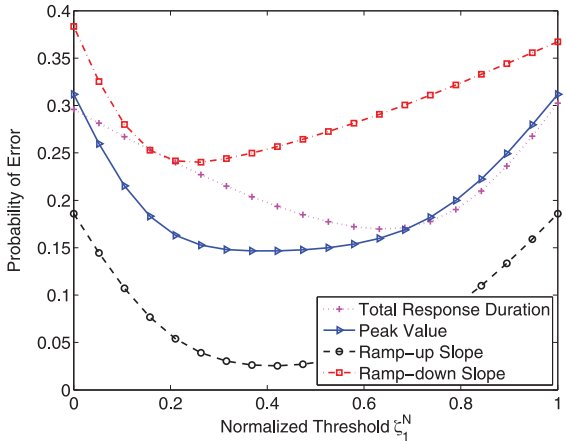

(a)

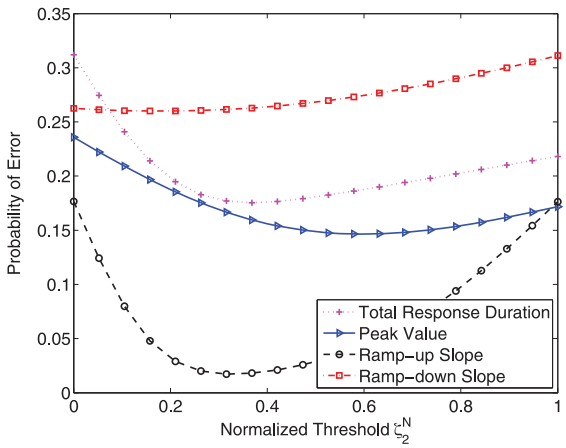

(b)

Fig. 12. Comparison of the sampling schemes with respect to probability of error for 3-ary PAM with 50 mins pulse width. Thresholds ζ_1 and ζ_2 are varied. To present results for different sampling schemes in the same plot, the thresholds ζ_1 and ζ_2 are normalized using $\zeta_1^N = (\zeta_1 - \mu_1)/(\mu_2 - \mu_1)$ and $\zeta_2^N = (\zeta_2 - \mu_2)/(\mu_3 - \mu_2)$, respectively.

TABLE VI
MINIMUM PROBABILITY OF ERROR FOR 3-ARY PAM

Sampling Scheme	ζ_1 varied, $\zeta_2^N = 0.5$	ζ_2 varied, $\zeta_1^N = 0.5$
Total Response Duration	0.1696	0.1755
Peak Value	0.1466	0.1465
Ramp-up Slope	0.0254	0.0172
Ramp-down Slope	0.2403	0.26

but later than the ramp-up behavior. The ramp-up slope provides the earliest opportunity for instantaneous detection purposes, since the bacteria response enters first to this behavior after it starts. The required observation durations for the different sampling strategies of the received signal are summarized as

$$\tau_{\text{total-response}} > \tau_{\text{ramp-down}} > \tau_{\text{peak}} > \tau_{\text{ramp-up}} \tag{26}$$

where $\tau_{\text{total-response}}$, $\tau_{\text{ramp-down}}$, τ_{peak}, and $\tau_{\text{ramp-up}}$ represent the required observation duration for the received signal sampling based on the total response duration, the ramp-down slope, the peak value, and the ramp-up slope, respectively. Next, we further investigate the detection of molecular signals using the ramp-up slope.

V. DETECTION OF MOLECULAR SIGNALS VIA RAMP-UP SLOPE OF THE BACTERIAL SIGNAL TRANSDUCTION

During the course of this work, we have found the following answers to the questions listed in the introduction section through both analytical and experimental investigation:

- The input-output relation of the signal transduction is one-to-one for sufficiently small input ranges. (Section II.B).
- The noise in the bacteria response scales directly proportional to the time elapses until the response reaches peak. Then, the noise reduces as the bacteria response decays (Section II.B and Section III.C).
- The time delay for the response beginning, the peak instant, and the response ending are shown to be randomly varying (Section III.B).
- The sampling based on the ramp-up slope is shown to be favorable according to the comparisons based on the p-values and the probability of error for the detection of binary and 3-ary PAM molecular signals (Section IV.B and Section IV.C).

Motivated by the results of comparisons based on p-test and probability of error, we further study the detection of molecular signals by sampling the raw bacteria response via the ramp-up slope.

A. Decision

We consider the use of t-test for the decision on whether a specific input level $\mathcal{H}_i$ is transmitted. μ_i corresponds to the mean of the sampled received signal for each input pulse level $\mathcal{H}_i$. Considering multiple repeated experiments, the t-statistic ξ is given by

$$\xi_i = \frac{\overline{r}_{\text{up}} - \mu_i}{s/\sqrt{K}} \tag{27}$$

where K is the number of samples, $\overline{x}$ is the sample mean given by

$$\overline{r}_{\text{up}} = \frac{1}{K}\sum_{k=1}^{K} r_{\text{up}}[k] \tag{28}$$

and s is the sample standard deviation given by

$$s = \sqrt{\frac{1}{K}\sum_{k=1}^{K}(r_{\text{up}}[k] - \mu_i)^2}. \tag{29}$$

The signal level $\mathcal{H}_i$ corresponding to the μ_i providing the minimum t-statistic ξ_i is decided as the input molecular signal.

B. Time Interval Selection for Ramp-Up Slope

The selection of time interval in bacteria response for the calculation of the mean ramp-up slope is of critical importance. In Fig. 4, it is observed that the instants when bacteria response enters and leaves ramp-up region vary based on input level. Furthermore, based on the results presented in Fig. 5, standard deviation of the bacteria response increases with the evolving time during the ramp-up behavior. Moreover, in Section II.B, it is

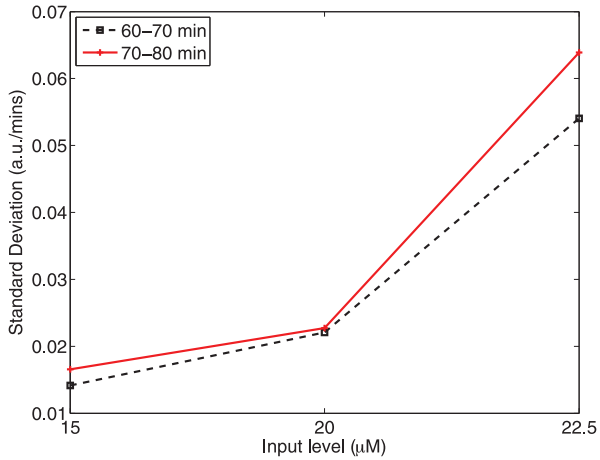

Fig. 13. Standard deviation of ramp-up slope with respect to input level for different time interval selections.

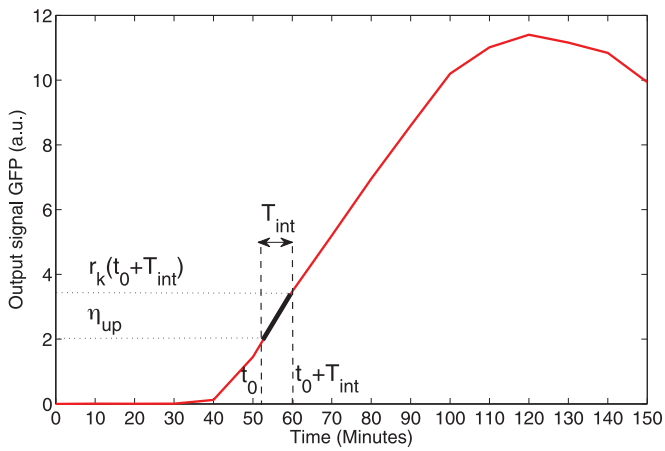

Fig. 14. The sampling of the raw bacteria response for the ramp-up slope $r_{\mathrm{up}}[k]$ (the raw bacteria response curve is taken from an individual experiment for 20 μM input).

shown analytically that the error is amplified with the evolving time during the ramp-up behavior. This suggests the earlier calculation of the ramp-up slope μ_i during the ramp-up behavior.

For different intervals, the standard deviation of the ramp-up slope is studied in Fig. 13. T_{int} is taken as 10 min, and the ramp-up slope is calculated for 60–70 min, and 70–80 min. It is shown that the standard deviation of the ramp-up slope is less for earlier intervals of bacteria response, e.g., 60–70 min interval has a lower standard deviation compared to the 70–80 min interval.

C. Non-Coherent Sampling for the Ramp-Up Slope

While earliest calculation of the ramp-up slope provides better prediction of the input level, the randomness in entering the ramp-up behavior yield strict timing requirements for detection impractical. Therefore, a non-coherent scheme for detection of molecular signals via bacteria response is needed to mitigate delay uncertainty and eliminate timing requirements at the receiver. To remove timing requirement for sampling, a differential detection scheme can be utilized, which is illustrated in Fig. 14. A sufficiently large threshold level η_{up}, for

1: **if** $r_k(t) == \eta_{up}$ **then**
2: $t_0 = current\ time$
3: **while** $t \leq t + T_{int}$ **do**
4: **if** $t = T_{int}$ **then**
5: $r_{up}[k] = \frac{r_k(t_0 + T_{int}) - \eta_{up}}{T_{int}}$
6: **end if**
7: **end while**
8: **end if**

Fig. 15. Non-coherent calculation of the ramp-up slope $r_{\mathrm{up}}[k]$.

which all different input levels i enter to the ramp-up region, can be determined, and the instant t_0 bacteria response reaches $r_{\mathrm{up}}(t_0) = \eta_{\mathrm{up}}$ level can be recorded. After waiting for the interval duration T_{int}, another sample can be taken from the response $r_k(t_0 + T_{\mathrm{int}})$. Accordingly, the ramp-up slope can be calculated, and t-test can be applied to detect the transmitted signal level. The proposed algorithm is summarized in Fig. 15.

VI. Conclusion

We have investigated the utilization of the bacterial signal transduction for the detection of pulse-amplitude modulated (PAM) molecular signals. The one-to-one input-output relation, the noise, and the timing issues on the bacteria response are examined based on both the measurements from the experiments and the analytical evaluations of a biochemical model of bacteria signal transduction. To sample the raw bacteria response, four different strategies, i.e., the total response duration, the peak value, the ramp-up slope, and the ramp-down slope, are statistically compared. Based on the statistical comparisons, the sampling of the bacteria response via the ramp-up slope is selected for further investigation. The time-interval selection and non-coherent sampling for ramp-up slope calculation from the raw bacteria response are studied to address noise and timing issues, respectively. The provided analyses and results in this work provide a basis for efficient detection of the PAM molecular signals in molecular communication and sensing applications.

Acknowledgment

The authors would like to thank J. Perdomo and S. Patel for their help with the experimental measurements.

References

[1] I. F. Akyildiz, F. Brunetti, and C. Blazquez, "Nanonetworks: A new communication paradigm," *Comput. Netw.*, vol. 52, no. 12, pp. 2260–2279, Aug. 2008.
[2] I. F. Akyildiz, F. Fekri, R. Sivakumar, C. R. Forest, and B. K. Hammer, "MONACO: Fundamentals of molecular nano-communication networks," *IEEE Wireless Commun.*, vol. 19, no. 5, pp. 12–18, Oct. 2012.
[3] T. Danino, O. Mondragon-Palomino, L. Tsimring, and J. Hasty, "A synchronized quorum of genetic clocks," *Nature*, vol. 463, no. 7279, pp. 326–330, Jan. 2010.
[4] S. Park, X. Hong, W. S. Choi, and T. Kim, "Microfabricated ratchet structure integrated concentrator arrays for synthetic bacterial cell-to-cell communication assays," *Lab. Chip*, vol. 12, no. 20, pp. 3914–3922, Sep. 2012.
[5] A. Prindle, J. Selimkhanov, H. Li, I. Razinkov, L. S. Tsimring, and J. Hasty, "Rapid and tunable post-translational coupling of genetic circuits," *Nature*, vol. 508, no. 7496, pp. 387–391, Apr. 2014.

[6] B. Krishnaswamy, C. M. Austin, J. P. Bardill, D. Russakow, G. L. Holst, B. K. Hammer, C. R. Forest, and R. Sivakumar, "Time-elapse communication: Bacterial communication on a microfluidic chip," *IEEE Trans. Commun.*, vol. 61, no. 12, pp. 5139–5151, Dec. 2013.
[7] S. J. Sorensen, M. Burmolle, and L. H. Hansen, "Making bio-sense of toxicity: New developments in whole-cell biosensors," *Current Opin. Biotechnol.*, vol. 17, no. 1, pp. 11–16, Feb. 2006.
[8] S. Belkin, "Microbial whole-cell sensing systems of environmental pollutants," *Current Opin. Microbiol.*, vol. 6, no. 3, pp. 206–212, Jun. 2003.
[9] T. Elad, J. H. Lee, M. B. Gu, and S. Belkin, "Microbial cell arrays," *Adv. Biochem. Engin/Biotechnol.*, vol. 117, pp. 85–108, 2010.
[10] J. R. van der Meer and S. Belkin, "Where microbiology meets microengineering: Design and applications of reporter bacteria," *Nature Rev. Microbiol.*, vol. 8, no. 7, pp. 511–522, 2010.
[11] C. M. Austin, W. Stoy, P. Su, M. C. Harber, J. P. Bardill, B. K. Hammer, and C. R. Forest, "Modeling and validation of autoinducer-mediated bacterial gene expression in microfluidic environments," *Biomicrofluidics*, 2014.
[12] M. Pierobon and I. F. Akyildiz, "A physical end-to-end model for molecular communication in nanonetworks," *IEEE J. Sel. Areas Commun.*, vol. 28, no. 4, pp. 602–611, May 2010.
[13] M. Pierobon and I. F. Akyildiz, "Diffusion-based noise analysis for molecular communication in nanonetworks," *IEEE Trans. Signal Process.*, vol. 59, no. 6, pp. 2532–2547, Jun. 2011.
[14] A. O. Bicen and I. F. Akyildiz, "System-theoretic analysis and least-squares design of microfluidic channels for flow-induced molecular communication," *IEEE Trans. Signal Process.*, vol. 61, no. 20, pp. 5000–5013, Oct. 2013.
[15] A. O. Bicen and I. F. Akyildiz, "End-to-end propagation noise and memory analysis for molecular communication over microfluidic channels," *IEEE Trans. Signal Process.*, vol. 62, no. 7, pp. 2432–2443, May 2014.
[16] M. Pierobon and I. F. Akyildiz, "Capacity of a diffusion-based molecular communication system with channel memory and molecular noise," *IEEE Trans. Inf. Theory*, vol. 59, no. 2, pp. 942–954, Feb. 2013.
[17] A. O. Bicen and I. F. Akyildiz, "Interference modeling and capacity analysis for microfluidic molecular communication channels," *IEEE Trans. Nanotechnol.*, vol. 14, no. 3, pp. 570–579, May 2015.
[18] B. Atakan and O. B. Akan, "Deterministic capacity of information flow in molecular nanonetworks," *Nano Commun. Netw.*, vol. 1, no. 1, pp. 31–42, Mar. 2010.
[19] D. Kilinc and O. B. Akan, "Receiver design for molecular communication," *IEEE J. Sel. Areas Commun.*, vol. 31, no. 12, pp. 705–714, Dec. 2013.
[20] L.-S. Meng, P.-C. Yeh, K.-C. Chen, and I. F. Akyildiz, "On receiver design for diffusion-based molecular communication," *IEEE Trans. Signal Process.*, vol. 62, no. 22, pp. 6032–6044, Nov. 15, 2014.
[21] H. H. McAdams and A. Arkin, "Stochastic mechanisms in gene expression," *Proc. Nat. Acad. Sci.*, vol. 94, pp. 814–819, Feb. 1997.
[22] M. Kaern, T. C. Elston, W. J. Blake, and J. J. Collins, "Stochasticity in gene expression: From theories to phenotypes," *Nature Rev.*, vol. 6, pp. 451–464, Jun. 2005.
[23] J. M. Raser and E. K. O'Shea, "Noise in gene expression: Origins, consequences, and control," *Science*, 2005.
[24] M. B. Elowitz, A. J. Levine, E. D. Siggia, and P. S. Swain, "Stochastic gene expression in a single cell," *Science*, 2002.
[25] U. Alon, *An Introduction to Systems Biology: Design Principles of Biological Circuits*. Boca Raton, FL, USA: CRC Press, 2006.
[26] R. Sharpeskhar, "Ultralow power bioelectronics," in *Fundamentals, Biomedical Applications and Bio-Inspired Systems*. Cambridge, U.K.: Cambridge Univ. Press, 2010.
[27] C. J. Myers, *Engineering Genetic Circuits*. London, U.K.: Chapman & Hall/CRC Press, 2010.
[28] G. Bernot, J.-P. Comet, A. Richard, M. Chaves, J.-L. Gouze, and F. Dayan, "Modeling and analysis of gene regulatory networks," in *Modeling in Computational Biology and Biomedicine*, F. Cazals and P. Kornprobst, Eds. New York, NY, USA: Springer, 2013, pp. 47–80.
[29] B. D. Unluturk, A. O. Bicen, and I. F. Akyildiz, "Genetically engineered bacteria-based biotransceivers for molecular communication," *IEEE Trans. Commun.*, vol. 63, no. 4, pp. 1271–1281, Apr. 2015.
[30] B.-S. Chen, W.-S. Wu, Y.-C. Wang, and W.-H. Li, "On the robust circuit design schemes of biochemical networks: Steady-state approach," *IEEE Trans. Biomed. Circuits Syst.*, vol. 1, no. 2, pp. 114–132, Jun. 2007.
[31] B.-S. Chen and P.-W. Chen, "Robust engineered circuit design principles for stochastic biochemical networks with parameter uncertainties and disturbances," *IEEE Trans. Biomed. Circuits Syst.*, vol. 2, no. 2, pp. 114–132, Jun. 2008.
[32] F.-X. Wu, "Global and robust stability analysis of genetic regulatory networks with time-varying delays and parameter uncertainties," *IEEE Trans. Biomed. Circuits Syst.*, vol. 5, no. 4, pp. 391–398, Aug. 2011.
[33] A. Bar-Even, J. Paulsson, N. Maheshri, M. Carmi, E. O'Shea, Y. Pilpel, and N. Barkai, "Noise in protein expression scales with natural protein abundance," *Nature Genetics*, vol. 38, no. 6, pp. 636–643, Jun. 2006.
[34] J. H. McDonald, *Handbook of Biological Statistics*, 3rd ed. Baltimore, MD, USA: Sparky House , 2014.
[35] H. L. Van Trees, *Detection, Estimation, and Modulation Theory, Part I*. New York, NY, USA: Wiley, 1968.

A. Ozan Bicen (S'08) received the B.Sc. degree from Middle East Technical University, Ankara, Turkey, and the M.Sc. degree in electrical and electronics engineering from Koc University, Istanbul, Turkey, in 2010 and 2012, respectively.

Currently, he is a Graduate Research Assistant in the Broadband Wireless Networking Laboratory and working toward the Ph.D. degree at the School of Electrical and Computer Engineering, Georgia Institute of Technology, Atlanta, GA, USA. His current research interests include molecular communication and nanonetworks.

Caitlin M. Austin received the B.S. degree in mechanical engineering from the Georgia Institute of Technology, Atlanta, GA, USA.

She was awarded the Nation Science Foundation Graduate Fellowship and is currently working toward the Ph.D. degree in bioengineering at the Georgia Institute of Technology. Her research interests include microfluidics and bacteria communication.

Ian F. Akyildiz (M'86–SM'89–F'96) received the B.S., M.S., and Ph.D. degrees in computer engineering from the University of Erlangen-Nurnberg, Erlangen, Germany, in 1978, 1981, and 1984, respectively.

Currently, he is the Ken Byers Chair Professor in Telecommunications in the School of Electrical and Computer Engineering, Georgia Institute of Technology (Georgia Tech), Atlanta, GA, USA. Also, he is the Director of the Broadband Wireless Networking Laboratory and Chair of the Telecommunication Group at Georgia Tech. He is an Honorary Professor in the School of Electrical Engineering at Universitat Politecnica de Catalunya (UPC), Barcelona, Catalunya, Spain. He founded the NaNoNetworking Center (N3Cat) in Catalunya. In addition, he is an Honorary Professor in the Department of Electrical, Electronic and Computer Engineering, University of Pretoria, Pretoria, South Africa, and founder of the Advanced Sensor Networks Lab. Since September 2012, he is a FiDiPro Professor [Finland Distinguished Professor Program (FiDiPro) supported by the Academy of Finland] in the Department of Communications Engineering, Tampere University of Technology, Tampere, Finland. His current research interests are in nanonetworks, Long Term Evolution (LTE) advanced networks, cognitive radio networks, and wireless sensor networks.

Dr. Akyildiz is the Editor-in-Chief of the *Computer Networks Journal* and the founding Editor-in-Chief of the *Ad Hoc Networks Journal*, *Physical Communication Journal*, and *Nano Communication Networks Journal*. He has been an ACM Fellow since 1997. He has received numerous awards from the IEEE and ACM.

Craig R. Forest received the B.S. degree in mechanical engineering from the Georgia Institute of Technology (Georgia Tech), Atlanta, GA, USA, in 2001, and the M.S. and Ph.D. degrees in mechanical engineering from the Massachusetts Institute of Technology, Cambridge, MA, USA, in 2003 and 2007, respectively.

Currently, he is an Associate Professor of Mechanical Engineering at Georgia Tech, where he also holds program faculty positions in bioengineering and biomedical engineering. He conducts research on miniaturized, high-throughput robotic instrumentation to advance neuroscience and genetic science, working at the intersection of bioMEMS, precision machine design, optics, and microfabrication. Prior to Georgia Tech, he was a Research Fellow in genetics at Harvard Medical School, Boston, MA, USA. He is cofounder/organizer of one of the largest undergraduate invention competitions in the U.S.—The InVenture Prize, and founder/organizer of one of the largest student-run prototyping facilities in the U.S.—The Invention Studio. Recently, he was a Fellow in residence at the Allen Institute for Brain Science, Seattle, WA, USA.

Dr. Forest he was awarded the Georgia Tech Institute for BioEngineering and BioSciences Junior Faculty Award (2010) and was named Engineer of the Year in Education for the state of Georgia (2013). He is one of the inaugural recipients of the NIH BRAIN Initiative Grants, a national effort to invent the next generation of neuroscience and neuroengineering tools. In 2007, he was a finalist on the ABC reality TV show "American Inventor."